Received: 13 December 2025 | Revised: 10 March 2026 | Accepted: 24 March 2026 | Published online: 13 April 2026

RESEARCH ARTICLE

Archives of Advanced Engineering Science
2026, Vol. 00(00) 1-16
DOI: 10.47852/bonviewAAES62028673

BON VIEW PUBLISHING

Numerical Investigation of Low-Frequency Sound Absorption in Micro-Perforated Panel–Porous Composite Structures

Majid Mohammadi[1,*] and Armin Hashemi[2]

[1] *School of Materials and Mineral Resources Engineering, Universiti Sains Malaysia, Malaysia*

[2] *Department of Mechanical Engineering, Isfahan University of Technology, Iran*

Abstract: This study conducts a numerical analysis of low-frequency sound absorption in micro-perforated panels (MPPs) and porous composites using the finite element method within COMSOL Multiphysics 6.2. The primary aim is to optimize the acoustic performance of MPP-based composite structures by systematically refining key design parameters, including hole diameter, perforation ratio, panel thickness, and air gap depth in combination with a porous layer. The research follows a multi-phase approach to evaluate the effects of these parameters and their interactions in various configurations. First, the influence of MPP characteristics on sound absorption coefficient was examined with a focus on optimizing to achieve maximum performance. Second, the integration of porous composite layers with MPPs in two distinct stacking configurations was explored: one with the porous layer placed behind and in front of the MPP. The third phase investigated the role of an air layer, analyzing the effects of varying its thickness and positioning to optimize impedance matching and enhance low-frequency sound absorption. Additionally, the impact of an additional air gap between layers was examined to identify configurations that maximize broadband absorption. The findings reveal that a strategic combination of MPPs, porous composites, and optimally positioned air gaps significantly enhances low-frequency sound absorption (50–1000 Hz). Results indicate that fine-tuning MPP perforation characteristics, in conjunction with carefully selected porous materials and well-calibrated air gaps, leads to a marked improvement in overall absorption efficiency. This study establishes a novel framework for designing high-performance acoustic panels, offering innovative solutions for noise control in architectural, transportation, and industrial applications.

Keywords: low-frequency sound absorption, micro-perforated panels (MPP), finite element method (FEM), COMSOL, Delany–Bazley model

1. Introduction

In today's rapidly advancing world, noise pollution has become a critical issue affecting both developed and developing countries, with significant consequences for human health and productivity [1]. The effects of noise pollution are wide-ranging, including increased stress, cognitive decline, sleep problems, heart conditions, restlessness, and elevated blood pressure [2–4]. A common approach to reducing environmental noise involves the use of sound absorbers. Acoustic absorbers are categorized into porous, Helmholtz, and panel (or membrane) types, with porous absorbers standing out for their cost-efficiency and high absorption performance [5]. Fiber-based materials utilized in porous sound absorbers are broadly categorized into natural and synthetic fibers. While synthetic fibers demonstrate superior sound absorption at higher frequencies (above 2000 Hz), growing environmental and health concerns have driven research toward sustainable natural fiber alternatives [6, 7]. Natural fibers not only provide effective acoustic absorption but also offer advantages such as lightweight characteristics, environmental sustainability, and safety, making them an attractive choice for acoustic applications [8, 9]. However, a significant limitation of porous absorbers is their reduced efficiency in the low-frequency range (below 1000 Hz) [10], which encompasses critical noise sources such as industrial machinery, vehicular noise, and human speech (500–1000 Hz) [11]. Addressing low-frequency noise is particularly challenging due to its long wavelengths, necessitating absorbers with considerable thickness [12]. However, practical constraints, including spatial limitations and production costs, often make such solutions unfeasible. Moreover, fibrous porous materials present additional drawbacks, such as potential fiber shedding, making them unsuitable for sterile environments due to associated health risks. These materials are also vulnerable to fire, moisture, wind, and mechanical stress, further restricting their application in low-frequency indoor noise control [13, 14]. Various strategies, such as increasing the absorber thickness or introducing air gaps, have been explored to enhance low-frequency

***Corresponding author:** Majid Mohammadi, School of Materials and Mineral Resources Engineering, Universiti Sains Malaysia, Malaysia. Email: majidmohammadi@student.usm.my

absorption [15–17]. However, these approaches often conflict with the $\lambda/4$ principle. For instance, achieving efficient absorption at 300 Hz would require an impractically thick absorber of approximately 29 cm, underscoring the necessity for innovative material designs and structural modifications to improve acoustic performance in the low-frequency domain [18]. To enhance low-frequency sound absorption, researchers have increasingly explored micro-perforated panels (MPPs), an advanced class of sound absorbers [19, 20]. MPPs feature perforations ranging from 0.1 mm to 1 mm in diameter, which effectively dissipate acoustic energy by inducing air oscillations within the perforations [21]. This mechanism converts sound energy into heat through friction and thermal losses. The absorption performance of MPPs is governed by several key parameters, including perforation diameter, spacing, perforation ratio, panel thickness, cavity depth, and material composition [22]. The diameter of the perforations plays a crucial role in determining acoustic behavior, as each hole functions similarly to a miniature Helmholtz resonator [23]. Smaller perforations enhance energy dissipation through increased viscous and thermal interactions [24], improving high-frequency absorption but restricting the effective bandwidth [17]. Conversely, larger perforations lower the resonant frequency and broaden the absorption range, although peak efficiency may decrease. By optimizing perforation size distributions or implementing multilayered panel configurations, MPPs can be engineered to achieve wideband absorption. Another critical factor is the perforation ratio, which represents the proportion of the panel surface occupied by perforations. A higher perforation ratio enhances sound-wave interaction, thereby improving high-frequency absorption, while a lower ratio increases airflow resistance, benefiting low-frequency performance [25]. Achieving an optimal balance between these effects is essential for applications spanning low-frequency noise control in architectural acoustics to mid- and high-frequency attenuation in automotive and industrial settings. The panel thickness and cavity depth behind the MPP also significantly influence absorption characteristics. Thicker panels and deeper cavities facilitate low-frequency absorption by shifting resonance frequencies and accommodating longer wavelengths [26]. Conversely, thinner panels with shallower cavities are more effective for high-frequency noise control. Advanced configurations, such as multi-depth cavity structures, further enhance broadband absorption by integrating multiple resonance effects. Material properties are equally vital in MPP design, where lightweight, flexible materials are better suited for low frequencies [27]. High damping properties enhance energy dissipation, while porous structures allow deeper sound penetration, optimizing overall absorption efficiency. In this regard, natural fiber-reinforced polymer composites (NFRPCs) incorporating fibers present sustainable alternatives with customizable acoustic properties [28]. The integration of NFRPCs with MPP technology offers effective impedance matching and enhanced energy dissipation, making them highly suitable for environmentally friendly and efficient noise control applications.

The finite element method (FEM) is an essential computational tool for simulating and optimizing the acoustic performance of the MPPs and porous composites [29]. By enabling the detailed modeling of complex geometries and sound-wave interactions within materials, FEM provides valuable insights into the absorption characteristics of different configurations. Through the numerical solution of acoustic wave equations within a discretized model, FEM facilitates an in-depth understanding of key factors influencing sound absorption, including material properties, geometric parameters, and boundary conditions [30]. In the context of MPPs and porous composites, FEM simulations are particularly useful for evaluating the impact of design variables on acoustic efficiency, allowing researchers to refine panel structures and material compositions for optimal performance. The ability to analyze absorption characteristics across a broad frequency spectrum is especially beneficial for addressing the challenges associated with low-frequency sound mitigation. Additionally, FEM modeling reveals the fundamental physical mechanisms governing sound absorption, enhancing the understanding of how material structures and configurations contribute to overall acoustic behavior [31]. MPPs are considered an advanced alternative to conventional fiber-based sound absorbers. However, their absorption mechanism, primarily governed by Helmholtz resonance, often results in a limited frequency bandwidth and reduced efficiency. To address this limitation, researchers have explored various strategies to enhance the absorption range of MPPs, such as optimizing air cavity dimensions [32], employing dual-panel configurations [33], and modifying structural parameters. One promising approach involves integrating porous absorbers within the rear air cavity, which not only extends the effective absorption bandwidth but also enhances low-frequency performance [34, 35]. In recent years, there has been increasing interest in utilizing natural fibers as sustainable sound-absorbing materials.

This study examines the potential of combining natural fiber-reinforced composites (NFRCs) with MPP structures to enhance sound absorption, particularly in the sub-2500 Hz frequency range. The research focuses on evaluating the influence of innovative panel configurations on absorption performance by systematically varying parameters such as cavity depth, perforation size and ratio, and panel thickness. A simulated composite system is developed, incorporating an NFRC layer, an MPP layer, and an air gap. The study utilizes material properties of date palm fiber, as reported in Taban et al.'s [36] research, and conducts FEM-based simulations in COMSOL Multiphysics 6.2 for precise acoustic analysis. The primary objective is to assess how novel design configurations influence sound absorption efficiency. The findings of this study highlight the novelty of integrating NFRCs with MPP structures to achieve enhanced low-frequency sound absorption. Unlike previous studies that focused primarily on conventional materials or isolated MPP designs, this work systematically explores innovative panel configurations and parameter variations to optimize acoustic performance. The results provide practical guidance for designing sustainable, high-performance acoustic materials and demonstrate their potential applicability in architectural acoustics, transportation systems, and industrial noise control, thereby bridging the gap between simulation-driven research and real-world implementation.

2. Theoretical Framework

2.1. Acoustics theory

The Helmholtz equation describes wave propagation in a homogeneous medium in the frequency domain. A plane wave is given by:

$$\frac{\partial^2 p}{\partial x^2} = \frac{1}{c^2}\frac{\partial^2 p}{\partial t^2} \tag{1}$$

where p is the acoustic pressure and c is the speed of sound. This equation is derived from the linearized wave equation under the assumption of time-harmonic solutions. In acoustics, boundary conditions such as rigid walls, impedance surfaces,

or fluid-structure interfaces modify wave behavior, affecting absorption, reflection, and transmission. For porous materials, the Delany–Bazley model is coupled with the Helmholtz equation to account for viscous and thermal losses. The absorption coefficient (α) is determined using the following equation:

$$\alpha = 1 - |R|^2 \tag{2}$$

where R is the pressure reflection coefficient.

2.2. MPP theory

The concept of acoustic impedance in the MPPs was first introduced by Maa [37]. According to Maa's foundational research, the acoustic impedance and absorption coefficient of MPPs can be determined using the following equations:

$$Z_{MPP} = Z_{Resistance} + Z_{Reactance} = r + i\omega m \tag{3}$$

$$r = \frac{32\eta t}{\rho_0 c_0 d^2 \sigma}\left[\sqrt{1 + \frac{x^2}{32} + \frac{xd\sqrt{2}}{32} + \frac{xd\sqrt{2}}{8t}}\right] \tag{4}$$

$$m = \frac{t}{\sigma c_0}\left[1 + (9 + \frac{x^2}{2})^{-0.5} + \frac{0.85d}{t}\right] \tag{5}$$

$$x = \frac{d}{2}\sqrt{\frac{\omega\rho_0}{\eta}} \tag{6}$$

$$\alpha = \frac{4r}{(1+r)^2 + (\omega m - \cot(\omega D/c))^2} \tag{7}$$

In these equations, r and m represent resistance and reactance, respectively. The parameter ρ_0 denotes air density, while c_0 corresponds to the speed of sound in air. The angular frequency is given by ω, t signifies the thickness of the MPP, σ represents the perforation ratio, d refers to the perforation diameter, and η denotes air viscosity. As is evident, acoustic impedance consists of both real and imaginary components. The real part, known as resistance, accounts for the viscous dissipation occurring as air flows through the perforations, leading to frictional energy loss. In contrast, the imaginary component, referred to as reactance, relates to the inertial effects of the oscillating air mass within the perforations. The model proposed by Delany and Bazley (D&B) in 1970 was the first of its kind, offering a straightforward, rapid, and semi-empirical approach for estimating the surface characteristic impedance and propagation constant of porous materials based on flow resistivity [38]. This model was derived through power–law relationships obtained by curve-fitting extensive experimental data on fibrous materials. The following formulation is employed to approximate the acoustical properties of porous media:

$$k = \frac{\omega}{c_0}\left[1 + C_1(X)^{-C_2} - iC_3(X)^{-C_4}\right] \tag{8}$$

$$Z_c = \rho_0 c_0\left[1 + C_5(X)^{-C_6} - iC_7(X)^{-C_8}\right] \tag{9}$$

$$X = \frac{\rho_0 f}{\sigma} \tag{10}$$

where ρ_0 represents the density of air, c_0 is the speed of sound in air, Zc denotes the characteristic impedance, and Kc is the propagation constant. The variables f and ω correspond to frequency and angular frequency, respectively, while σ signifies the static airflow resistivity. Additionally, R represents the sound pressure reflection coefficient, Zs denotes the surface impedance, and d refers to the sample thickness. A limitation of Maa's theory is that it assumes the perforations are cylindrical and uniformly distributed across the panel [37]. While the model effectively predicts sound absorption performance based on panel properties and cavity depth, its accuracy diminishes when the micro- perforations vary in size or have irregular shapes [39].

2.3. Delany–Bazley model

While the D&B model remains a widely used approach for estimating the sound absorption coefficient (SAC) of various mineral and synthetic fibrous materials, its applicability is constrained by several limitations. Specifically, the model struggles to accurately predict the acoustic behavior of thicker natural fiber-based samples and has a restricted range of validity [40]. A key challenge lies in the precise measurement of airflow resistivity, which serves as the model's primary parameter. The porosity should be nearly 1, a condition met by most purpose-built fibrous absorbers ($0.01 < X < 1.0$), indicating that the formulations are applicable only within a specific frequency range [41]. In natural fiber composites, non-laminar airflow and minimal pressure differentials across the sample can complicate resistivity measurements, leading to deviations in absorption predictions. To address these shortcomings, researchers have proposed multiple refinements to enhance the model's predictive accuracy and extend its applicability to a broader range of materials. For example, Miki [42] and Komatsu [43] introduced constraints to the D&B model, ensuring physically meaningful values for the propagation coefficient and characteristic impedance while also refining the model's accuracy at lower frequencies. In this study, we adopt the best-fit inverse methodology introduced by Berardi et al. as a foundational approach to optimize the model coefficients (ci), where i = 1, 2, ..., 8). By fitting experimental results to the D&B equations, the optimized coefficients are derived using the Nelder–Mead simplex algorithm. Table 1 shows the optimized and original values of C1–C8 for this study. The parametric investigation process minimizes the squared difference between the measured and predicted absorption coefficients, yielding an error function that quantifies the model's accuracy.

Table 1
Optimized and original values of C1–C8

Coefficient	Optimized value	Original values
C_1	0.6399	0.0978
C_2	–0.6002	0.7
C_3	0.1987	0.189
C_4	0.5472	0.595
C_5	0.0003	0.0571
C_6	2.210	0.754
C_7	0.0662	0.087
C_8	0.8461	0.732

Figure 1
Schematic of the impedance tube with a fine default mesh

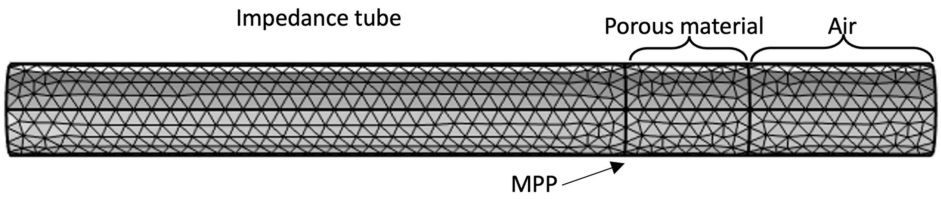

3. Research Methodology

3.1. Research design

The numerical simulations in this study were conducted using COMSOL Multiphysics 6.2, which employs the FEM to determine the SAC. A three-dimensional impedance tube model with a diameter of 30 mm and a length of 300 mm was developed using the pressure acoustics physics interface. The MPP was defined as an interior perforated plate boundary, while the porous material was represented using the poroacoustics domain, incorporating frequency-dependent effective fluid density $\rho(\omega)$ and bulk modulus $K(\omega)$ to describe the equivalent fluid–solid system. The incident pressure was applied through a circular port with a pressure amplitude of 1 Pa, and the porous material was backed by a rigid wall. Among the various poroacoustics models available in COMSOL, the Delany–Bazley–Miki model was selected, requiring only flow resistivity as input. The MPP simulation involved three key parameters: hole diameter, plate thickness, and area porosity, which were varied to obtain optimized results. The final configuration was chosen based on low-frequency performance constraints. Figure 1 illustrates the schematic of the impedance tube, incorporating a fine default mesh to ensure accurate simulation and analysis of sound absorption characteristics.

The study was conducted in three distinct phases to systematically analyze and optimize the acoustic performance of MPP structures combined with porous materials. In the first phase, the focus was on evaluating the influence of key MPP parameters, including perforation ratio, hole diameter, and panel thickness. These parameters were individually analyzed and then collectively optimized to identify the most effective configuration for sound absorption enhancement. The second phase examined the integration of the MPP layer with a porous absorber, considering two different configurations: one with the porous layer positioned behind the MPP and another with it placed in front. The thickness of the porous layer was selected based on the optimal sample identified in Taban et al.'s study [36] and was maintained constant throughout the analysis. This phase aimed to assess how various MPP design parameters influence the acoustic behavior of the porous absorber. In the third phase, the impact of an air gap on the absorption coefficient was explored by varying its thickness and placement within the system. The objective was to identify the most effective configuration for enhancing sound absorption, particularly in the low-frequency range while maintaining broad bandwidth performance. The specifications and values of the parameters investigated in this study are summarized in Table 2. Figure 2 provides a visual representation of all the configurations for FEM modeling.

Table 2
Specifications and values of each parameter

Parameters	Values
Hole diameter (mm)	0.7, 0.8, 0.9, 1
Perforation ratio (%)	0.1, 0.5, 1, 1.5, 2
MPP thickness (mm)	0.5, 1, 1.5, 2, 2.5, 3
Thickness of porous layer (mm)	40 (constant)
Air gap thickness (mm)	10, 20, 30, 40, 50, 60

Figure 2
Visual representation of all the configurations for FEM modeling

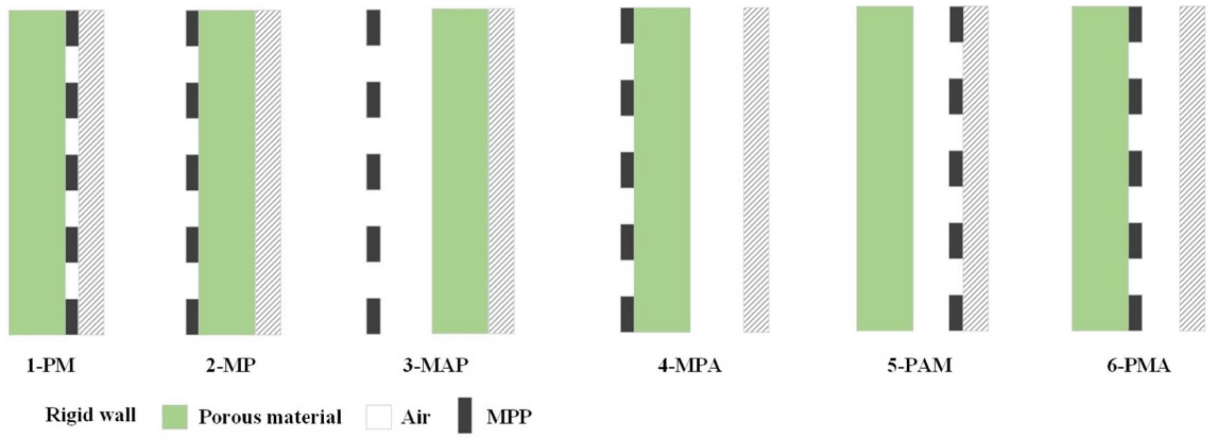

4. Result and Discussion

4.1. The MPP structure

Figure 3 illustrates parameters affecting sound absorption properties of the MPP structure, including panel thickness, hole diameter, and perforation ratio, as well as parametric investigation of all parameters altogether, focusing on frequencies below 2500 Hz. Figure 3(a) provides a detailed depiction of how variations in hole diameter affect the acoustic performance of the MPP. The data reveal that smaller hole diameters enhance both the absorption peak and the overall performance at lower frequencies, suggesting a direct correlation between reduced hole size and a higher resonance peak. Conversely, increasing the hole diameter diminishes the absorption coefficient and weakens the resonance peak. These findings underscore the critical role of hole diameter as a key parameter significantly influencing the behavior of the MPPs. Therefore, accurate determination of hole dimensions is essential to achieve the desired acoustic properties. As illustrated in Figure 3(b), an increase in the perforation ratio of the panel induces a shift in the resonance frequency toward higher frequencies, concomitantly increasing absorption at those higher frequencies. Conversely, a reduction in the perforation ratio leads to an increase in the absorption peak, causing it to transition toward lower frequencies. To clarify, at a frequency of 500 Hz, panels with perforation ratios of 0.5 and 1% exhibit absorption coefficients of over 0.9 and 0.8, respectively. Interestingly, the reduction in the percentage of perforation enhances absorption at lower frequencies, whereas an augmentation in the perforation ratio improves absorption at higher frequencies. It is noteworthy that this manipulation primarily affects the bandwidth rather than altering the peak amplitude. Thus, the study underscores the critical importance of selecting an appropriate perforation ratio to attain the desired bandwidth and optimal absorption range. As depicted in Figure 3(c) increasing the panel thickness is associated with an elevation in the resonance peak and heightened absorption at low frequencies, albeit at the cost of a narrower overall bandwidth. Conversely, reducing panel thickness leads to a diminished resonance peak and a smoother graph. For instance, at a frequency of 400 Hz, a composite with a thickness of 0.5 mm exhibits an absorption coefficient of 0.1, whereas a thickness of 3 mm yields an absorption coefficient of 1, which is primarily due to the enhanced interaction between the sound wave and the material. On the other hand, at a frequency of 1000 Hz, a composite with a thickness of 0.5 mm exhibits an absorption coefficient of 0.5, whereas a thickness of 3 mm yields an absorption coefficient of 0.1. Unlike the hole diameter, which predominantly influences the resonance peak, the panel thickness appears to play a role in determining the bandwidth.

Figure 3
Influence of various parameters on the sound absorption coefficient of micro-perforated panels: (a) effect of hole diameter, (b) effect of perforation ratio, (c) effect of thickness of MPP, (d) parametric investigation

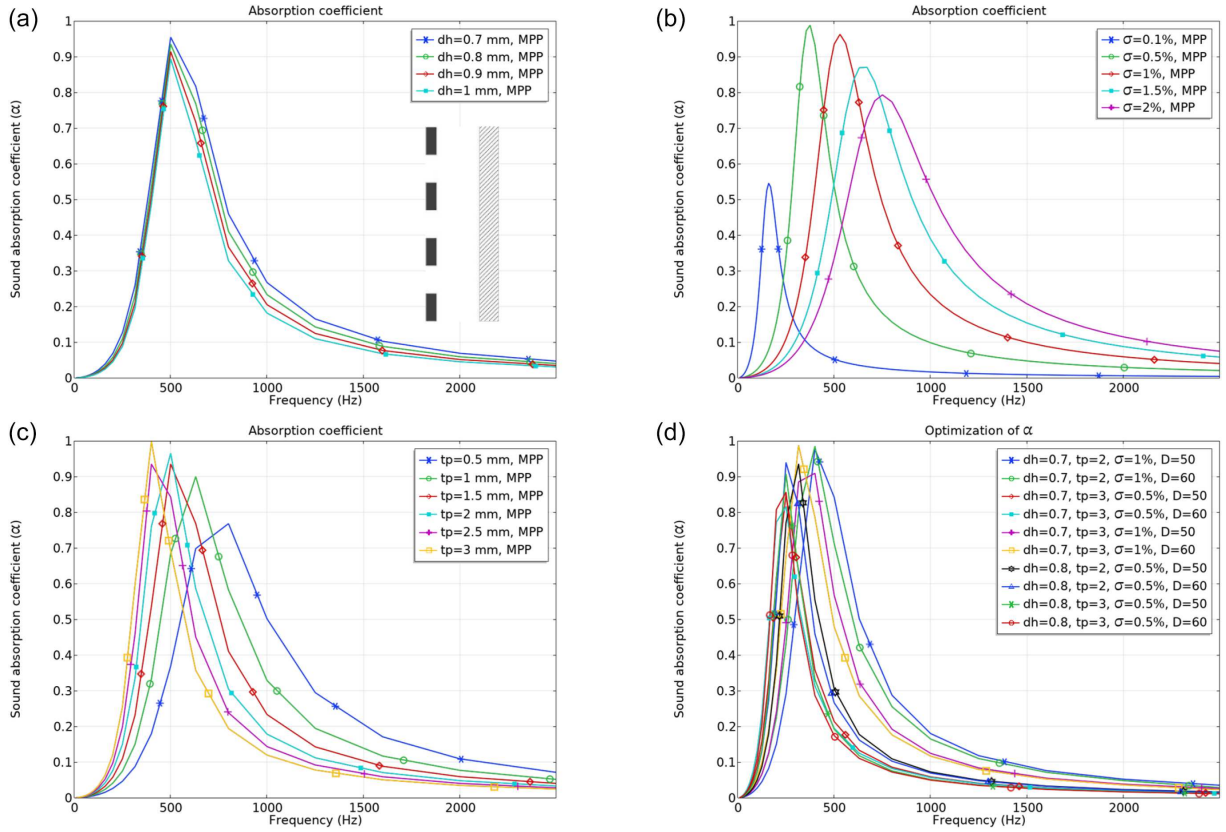

4.2. Effect of MPP and porous layer

Figure 4 investigates the influence of MPP parameters on the sound absorption performance of a composite system comprising a porous layer and an MPP, where the MPP is positioned behind the porous layer, ensuring that acoustic waves first interact with the porous material before reaching the MPP. The effect of each parameter was systematically analyzed, and a parametric investigation study was conducted to identify the best combination of parameters for enhanced sound absorption. The thickness of the porous layer was kept constant throughout the simulations (40 mm), focusing exclusively on the variations in MPP properties. The results provide insights into how different configurations of MPPs can change the acoustic performance of composite systems. As observed in all the graphs, the trends are consistent, confirming that integrating an MPP behind a porous material does not significantly enhance the SAC. Variations in hole diameter, perforation ratio, and panel thickness exhibit negligible influence on SAC, indicating that the MPP layer does not contribute meaningfully to the system's acoustic performance. Instead, the porous material remains the primary absorber, with its intrinsic properties governing the absorption characteristics. A 40 mm thick porous material exhibits superior absorption, particularly in the mid- to high-frequency range, achieving an average SAC of 0.7–0.9. However, the lack of performance improvement with the addition of MPP suggests that this structural configuration is acoustically ineffective. The consistent behavior across all cases implies that the MPP, in this arrangement, functions merely as a passive layer without actively enhancing sound dissipation. To achieve greater absorption efficiency, alternative configurations should be considered, such as embedding the MPP within the porous structure, introducing an optimized air gap to better interact with the acoustic wave propagation.

Figure 5 explores the impact of the MPP parameters on the SAC performance of a composite system, where the MPP is positioned in front of the porous material. In this configuration, acoustic waves interact with the MPP first before propagating through the porous layer to systematically analyze the effects of these parameters and optimize their combination for enhanced sound absorption. This configuration provides a unique insight into the interplay between the MPP and the porous layer, particularly in the absorption of low-frequency acoustic waves. Figure 5(a) depicts the influence of hole diameter on the SAC for an MPP positioned in front of a porous layer. Across the 0–500 Hz frequency range, the SAC exhibits a consistent trend, indicating that variations in dh have a negligible effect on absorption. However, at frequencies exceeding 700 Hz, minor differences emerge, with smaller hole diameters (dh = 0.7 mm) demonstrating slightly enhanced sound absorption performance. The perforation ratio significantly affects the acoustic performance, as depicted

Figure 4
Influence of MPP parameters on sound absorption performance of the first configuration (porous–MPP, PM) (the MPP is positioned behind the porous layer): (a) effect of hole diameter, (b) effect of perforation ratio, (c) effect of thickness of MPP, (d) parametric investigation

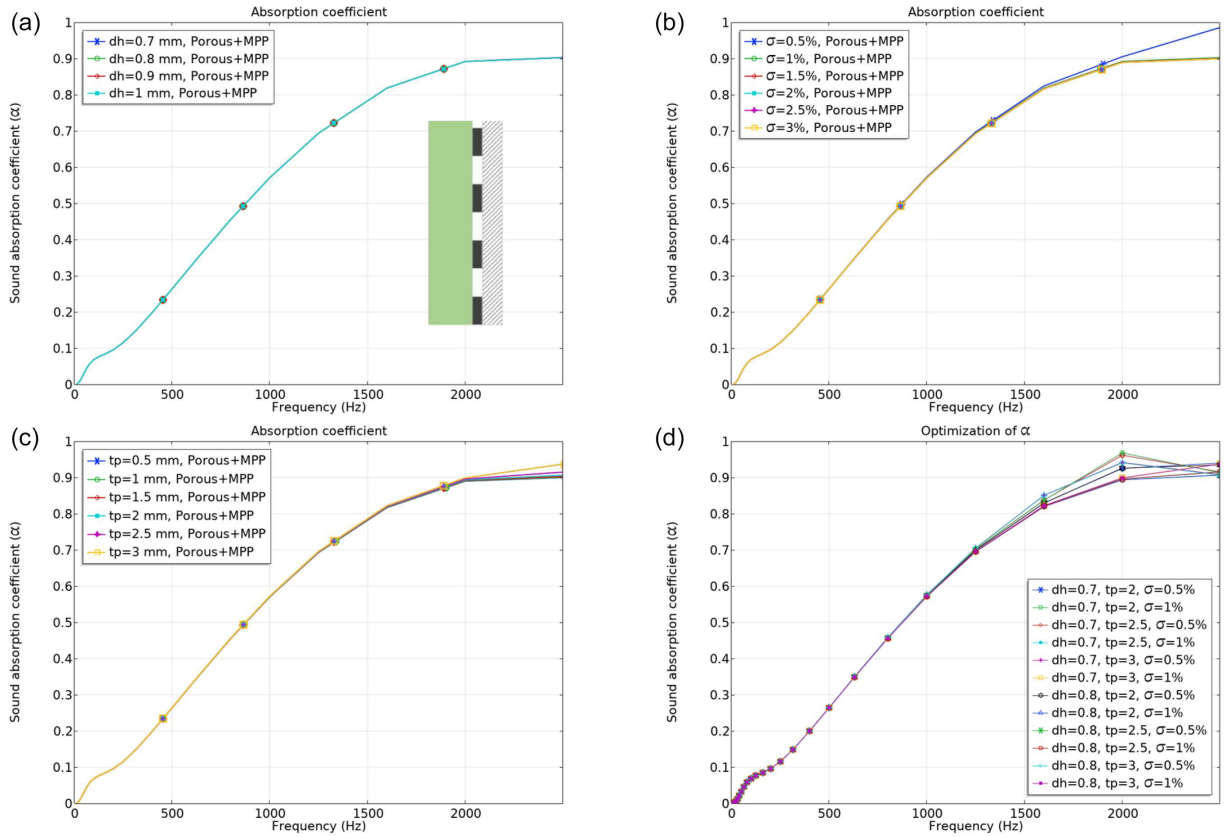

Figure 5

Influence of MPP parameters on sound absorption performance of the second configuration (MPP–porous, MP) (MPP is positioned in front of the porous material): (a) effect of hole diameter, (b) effect of perforation ratio, (c) effect of thickness of MPP, (d) parametric investigation

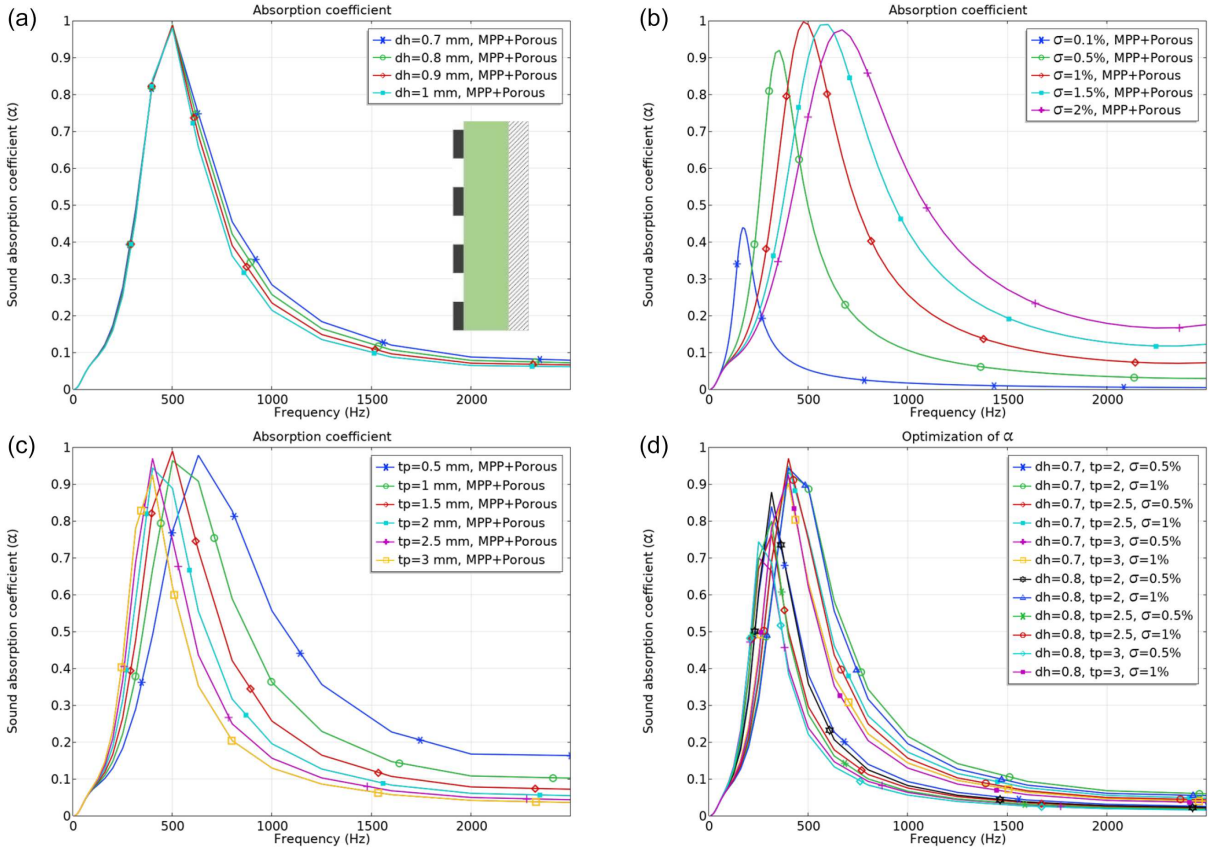

in Figure 5(b). A lower perforation ratio (σ = 0.5%) achieves the most prominent peak at low frequencies but shows a rapid decline at higher frequencies. In contrast, higher perforation ratios (σ = 2%) provide broader absorption at mid-frequencies compared to the low perforation and provide broader absorption across the mid-to-high range. A perforation ratio of 0.1 exhibits the lowest sound absorption across both low and high frequencies, with a peak absorption of approximately 0.4 at lower frequencies. This behavior is attributed to the insufficient interaction between the perforations and the acoustic wave, leading to reduced energy dissipation. The limited perforation restricts airflow resistance and viscous losses, resulting in suboptimal absorption performance across the frequency spectrum.

Figure 5(c) shows how varying the MPP thickness affects the absorption coefficient. Thicker panels demonstrate better absorption performance at lower frequencies, with a peak around 0–700 Hz. However, thinner panels (tp = 0.5 mm) show broader absorption peaks at mid to high frequencies. This phenomenon arises from the mass–air compliance effect and resonance behavior of the MPP. Thicker panels (tp = 3 mm) increase acoustic mass, lowering the resonance frequency and enhancing low-frequency absorption (0–500 Hz), while thinner panels have lower mass, shifting resonance to higher frequencies and providing broader absorption across the mid-to-high range. Figure 5(d) combines the effects of dh, tp, and σ to identify the optimal combination of parameters for maximum sound absorption. Smaller hole diameters (dh = 0.7 mm), intermediate panel thicknesses

Figure 6

Effect of air cavity depths on the sound absorption coefficient of MPP–air–porous structure, third configuration (MAP)

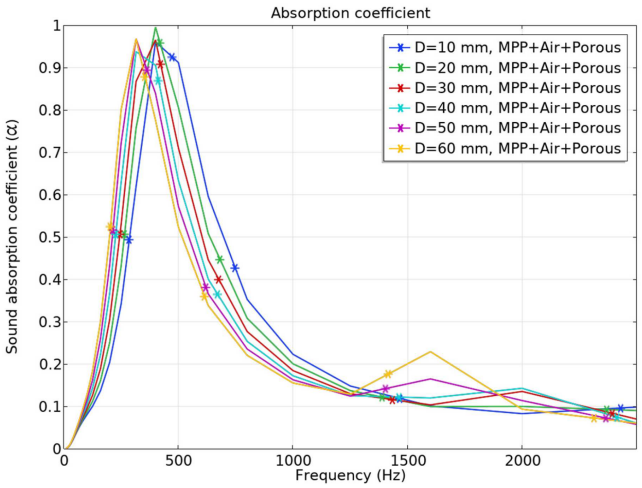

(tp = 2.5 mm), and moderate perforation ratios (σ = 0.5%) produce the best overall absorption, particularly at 0–500 Hz. The results emphasize the interdependence of these parameters in achieving desired acoustic performance. These findings provide a comprehensive understanding of how MPP parameters interact

with a porous layer when the MPP is placed in front, paving the way for further optimization of sound absorption systems. The two configurations of the MPP and porous layers display distinct sound absorption characteristics due to their unique layer configurations. When the MPP is positioned behind the porous material, the system achieves enhanced absorption in the mid- to high-frequency ranges. In this configuration, the porous layer directly interacts with the incoming sound waves, and the MPP's parameters have no significant effect on the SAC. Conversely, when the MPP is placed in front of the porous material, the system is more effective at absorbing low frequencies. The MPP utilizes resonant effects to modify the sound waves before they reach the porous layer. The choice of optimal configuration is application-dependent.

4.3. Effect of MPP, porous layer, and air gap

This section explores the impact of adding an air gap to MPP composites combined with porous layers. Four different air gap configurations will be analyzed to determine their effect on sound absorption performance across various frequencies, aiming to identify optimal designs for improved acoustic efficiency. Figure 6 shows the influence of cavity depth on the third configuration (MPP–air–porous, MAP), where the MPP is the first layer in contact with the sound energy, followed by the air gap and the porous layer.

The results demonstrate that cavity depth significantly influences the SAC, particularly in the low-frequency range. It can be observed that increasing the cavity depth shifts the peak absorption frequency toward lower frequencies, aligning with theoretical predictions based on acoustic impedance matching. The sample with a 20 mm cavity depth exhibits the highest peak absorption at low frequencies. A distinct peak in the SAC is observed between 400 and 600 Hz for all cavity depths, indicating optimal resonance conditions within this frequency range. This peak corresponds to the matching of acoustic impedance between the MPP structure and the surrounding medium. However, beyond this range (after 600 Hz), the SAC significantly decreases for all samples. This decline can be attributed to the reduced effectiveness of the resonance mechanism at higher frequencies, where the cavity no longer provides the optimal phase shift required for constructive interference of sound waves. The decrease in absorption after 600 Hz suggests that the cavity depth primarily influences the low-frequency absorption, while higher frequencies are less impacted by cavity variations. Figure 7 shows the third configuration (MAP) of the SAC with frequency for different air gap thicknesses in the configuration, where the MPP is the first layer in contact with the sound energy, followed by the air gap and the porous layer. The position of the back air gap in an MPP structure has a direct effect on determining the overall sound absorption performance, particularly in the low-frequency range. This configuration allows the sound waves to travel a longer path, increasing the chances of energy dissipation through viscous and thermal losses. The air gap acts as a resonant cavity, promoting Helmholtz resonance at low frequencies, where sound absorption is typically challenging. By positioning the air gap at the back, the structure

Figure 7
Sound absorption coefficient for MPP–air gap–porous layer with 10–60 mm air gaps (third configuration, MAP): (a) effect of hole diameter, (b) effect of perforation ratio, (c) effect of thickness of MPP, (d) parametric investigation

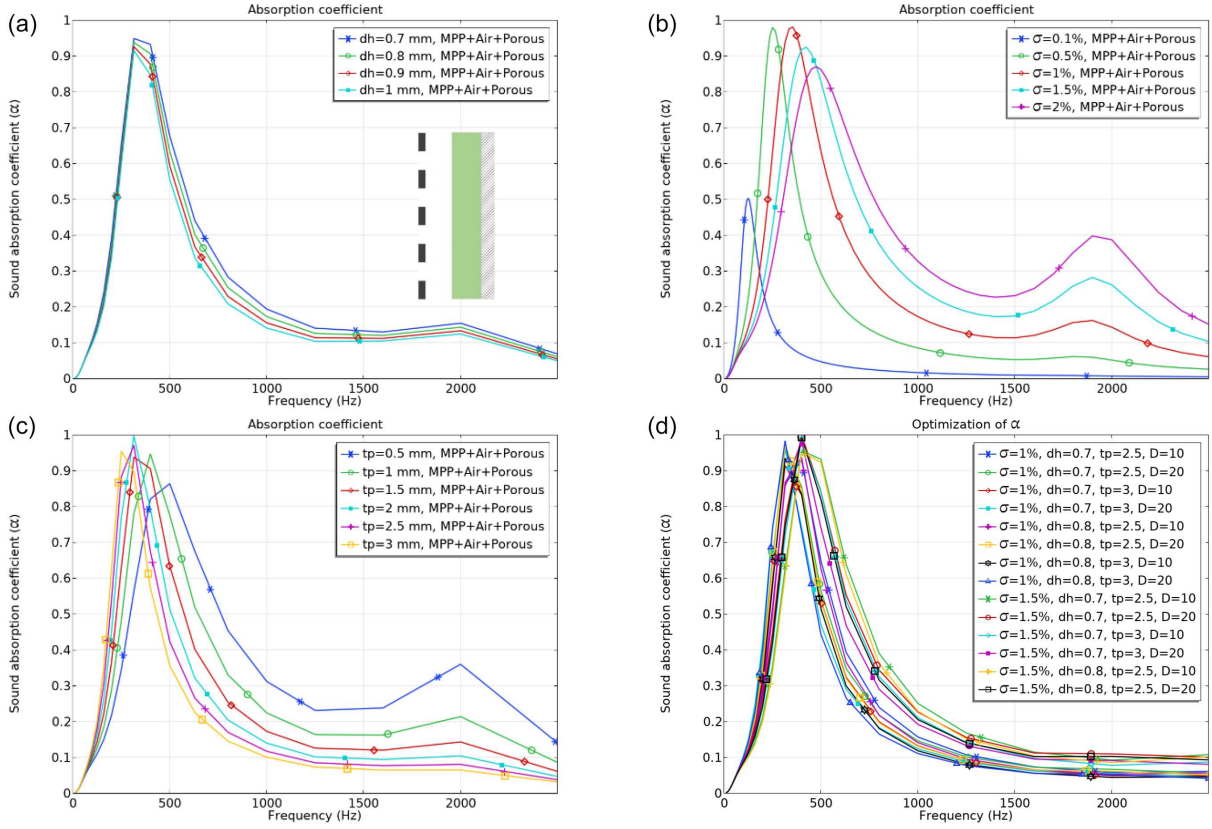

achieves better resonance effects, which amplifies the damping of acoustic energy and results in superior absorption performance in the low-frequency domain. Moreover, at higher frequencies, the air cavity contributes to the formation of standing waves, such as quarter-wavelength resonance, where the depth of the air gap matches specific sound wavelengths. This further boosts the absorption coefficient, ensuring efficient broadband sound attenuation. In summary, the strategic placement of the back air cavity is essential for optimizing the acoustic performance of MPP structures, as it enhances low-frequency resonance, promotes effective sound-wave interaction, and facilitates energy dissipation across a wider frequency range.

The effect of hole diameter on the SAC up to 500 Hz shows a consistent increasing trend with no significant alterations among different hole sizes (Figure 7(a)). This behavior indicates that, in the low-frequency range (below 500 Hz), the Helmholtz resonance effect, primarily governed by the air gap and MPP structure, dominates the absorption performance rather than the hole diameter itself. As the frequency approaches 500 Hz, the SAC reaches its peak value of approximately 0.95, indicating maximum sound absorption. This peak occurs due to the resonant interaction between the air cavity and the micro-perforations, where the acoustic mass and stiffness of the system align with the incident sound-wave frequency, resulting in efficient energy dissipation. After 500 Hz, there is a slight alteration in the SAC, with smaller hole diameters exhibiting slightly better absorption performance in the mid- to high-frequency range. Perforation ratios of 0.5% and 1% exhibit the highest SAC in the low-frequency range, reaching a peak of around 0.95, as depicted in Figure 7(b). This excellent low-frequency absorption results from a balanced interaction between acoustic resistance and Helmholtz resonance, which effectively dissipates sound energy. In contrast, perforation ratios of 1.5% and 2% provide enhanced absorption in the mid-frequency range, demonstrated by a broader SAC curve. The increased perforation ratio allows for greater airflow through the panel, leading to higher viscous losses and more efficient absorption across a wider frequency spectrum. On the other hand, a 0.1% perforation ratio shows the lowest absorption performance, with a maximum SAC of 0.5 observed only at low frequencies. The limited airflow caused by the small perforation area restricts energy dissipation, thereby reducing absorption at higher frequencies. An important trend emerges as the perforation ratio increases: the absorption peak shifts toward higher frequencies, indicating a frequency-dependent behavior. For instance, the 2% perforation ratio achieves a maximum SAC of 0.4 at 2000 Hz, demonstrating its effectiveness in high-frequency absorption. The thickness of the MPP has a significant impact on the SAC across different frequency ranges (Figure 7(c)). Based on the provided data, increasing the thickness leads to improved low-frequency sound absorption. Notably, the 2 mm thick sample achieves the highest SAC of 1.0 in the low-frequency region. However, this absorption peak is narrow, indicating that thicker panels primarily enhance absorption within a limited frequency range. In contrast, the 0.5 mm thick sample demonstrates a broader SAC curve, with a maximum SAC of 0.85 at 500 Hz. This suggests that thinner panels provide a wider frequency bandwidth for effective sound absorption. The broad absorption range of the 0.5 mm thickness sample distinguishes it from thicker configurations (1–3 mm), making it more suitable for applications where wideband absorption is desired. Additionally, in the high-frequency range (around 2000 Hz), the 0.5 mm thick panel maintains a SAC of 0.35, which is the highest value compared to the thicker samples. This superior performance at higher frequencies highlights the versatility

Figure 8
Effect of air cavity depths on the sound absorption coefficient of MPP–porous–air structure, fourth configuration, MPA

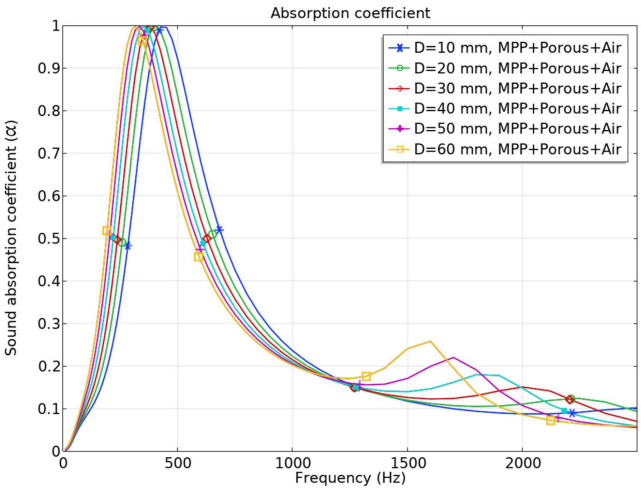

of thinner MPPs, offering broadband absorption that spans from mid to high frequencies.

Figure 8 shows the influence of cavity depth on the fourth configuration (MPP–porous–air, MPA), where the MPP is the first layer in contact with the sound energy, followed by the porous layer and the air gap. It is observed that increasing the cavity depth shifts the peak sound absorption frequency toward lower frequencies. Specifically, the sample with a 60 mm air gap achieves a SAC of 1.0 at 300 Hz, whereas the sample with a 10 mm air gap reaches the same SAC at 450 Hz. However, beyond 1250 Hz, the trend reverses, with samples having the largest air gap exhibiting higher SAC values, peaking at 0.25 at 1600 Hz.

Figure 9 depicts the fourth configuration (MPA) of sound absorption performance of multilayered structures consisting of an MPP as the first layer, a porous material as the second layer, and air gap thicknesses as the third layer. The position of the air gap has a direct role in determining the overall acoustic performance of the multilayer structure, especially in the low-frequency range. In the current configuration, where the air gap is positioned as the last layer (behind the porous material), there is a noticeable improvement in sound absorption at low frequencies compared to the third configuration, where the air gap was placed before the porous layer. This configuration follows a similar trend to the previous one, with a slight increase in SAC values. For instance, the effect of hole diameter on SAC up to 500 Hz shows a consistent upward trend across different hole sizes (Figure 9(a)). However, the maximum peak here is 1.0, compared to 0.95 in the previous configuration. The improved SAC is likely due to better impedance matching and increased acoustic energy dissipation. Regarding the perforation ratio, the trend remains the same (Figure 9(b)). The maximum SAC at low frequencies is 1.0 for a 1% perforation ratio, while at high frequencies (2000 Hz), it reaches 0.45. In contrast, the previous configuration showed maximum values of 0.98 and 0.4, respectively. The higher SAC values can be linked to enhanced airflow resistivity and improved absorption efficiency at both low and high frequencies. Similarly, the effect of thickness on SAC follows the same pattern (Figure 9(c)), with all thicknesses (1–3 mm) achieving a maximum SAC of 1.0, except for the 0.5 mm sample, which has a peak of 0.95, which is one unit higher than the previous configuration. The slight increase at high frequencies is also attributed to the greater damping effect

Figure 9
Sound absorption performance of fourth configuration (MPA) with varying air gap thicknesses (10–60 mm): (a) effect of hole diameter, (b) effect of perforation ratio, (c) effect of thickness of MPP, (d) parametric investigation

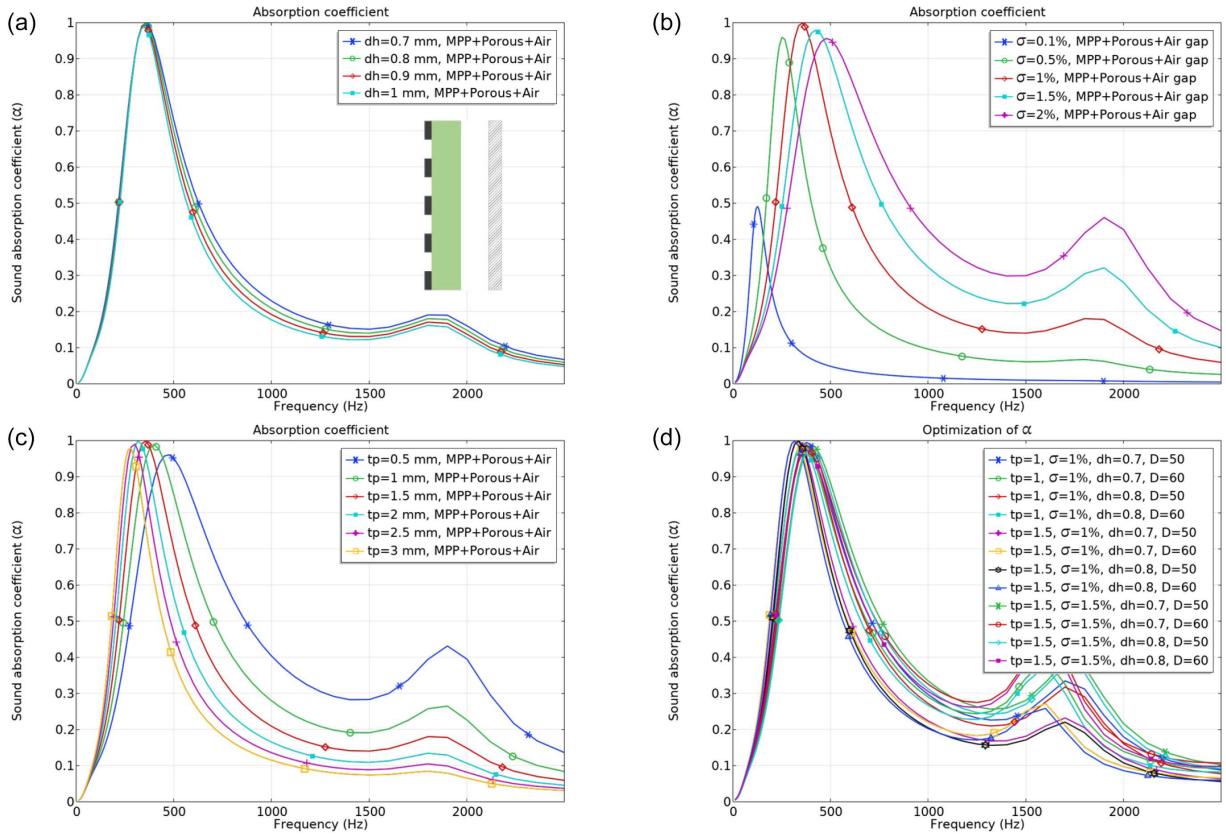

provided by the thicker samples. The most notable difference between this configuration and the previous one appears in the parametric investigation graph. In this structure, the SAC reaches up to 0.45 in the high-frequency range (1400–1700 Hz), whereas the previous structure showed no significant absorption after 1000 Hz, maintaining a constant SAC of 0.1. The porous layer, positioned between the MPP and the air gap, plays a critical role in dissipating energy via viscous and thermal losses. At higher frequencies, the increased interaction between the porous layer and the MPP perforations leads to effective damping of sound energy, amplifying the second peak. Configurations that combine thicker MPPs (1.5 mm) with medium perforation ratios (1%) and hole diameters (0.8 mm) achieve superior sound absorption. These combinations strike a balance between structural resonance, airflow resistance, and the dissipation of sound energy, effectively enhancing the system's ability to absorb sound.

Figure 10 illustrates the effect of cavity depth on a fifth configuration (porous–air–MPP, PAM) where the porous layer is positioned closest to the sound source, followed by the air gap and the MPP.

In general, the SAC increases with frequency for all air gap thicknesses, with prominent peaks appearing in the mid- to high-frequency ranges, reaching a maximum SAC of 0.9. The thickness of the air gap directly influences the frequency at which peak absorption occurs. At lower frequencies (below 1000 Hz), a larger air gap significantly improves sound absorption by shifting the absorption peaks toward lower frequencies. For example, the 60 mm air gap achieves the highest SAC of 0.9, while the 10 mm air gap shows the lowest SAC of 0.65. This

Figure 10
Effect of air cavity depths on the sound absorption coefficient of porous–air–MPP structure, fifth configuration (PAM)

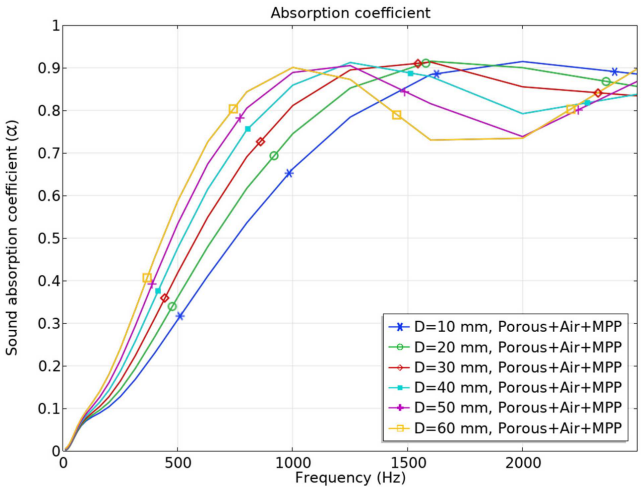

trend highlights the superior low-frequency performance of the 60 mm air gap compared to smaller gaps. In the mid-frequency range (1000–2500 Hz), all configurations maintain high SAC values with minimal differences among them, suggesting that the effect of the air gap is less pronounced in this region. Notably, air gaps of 40 mm and 50 mm consistently provide better absorption across a broad frequency range, indicating that these thicknesses

Figure 11
Sound absorption performance of fifth configuration (PAM) with varying air gap thicknesses (10–60 mm): (a) effect of hole diameter, (b) effect of perforation ratio, (c) effect of thickness of MPP, (d) parametric investigation

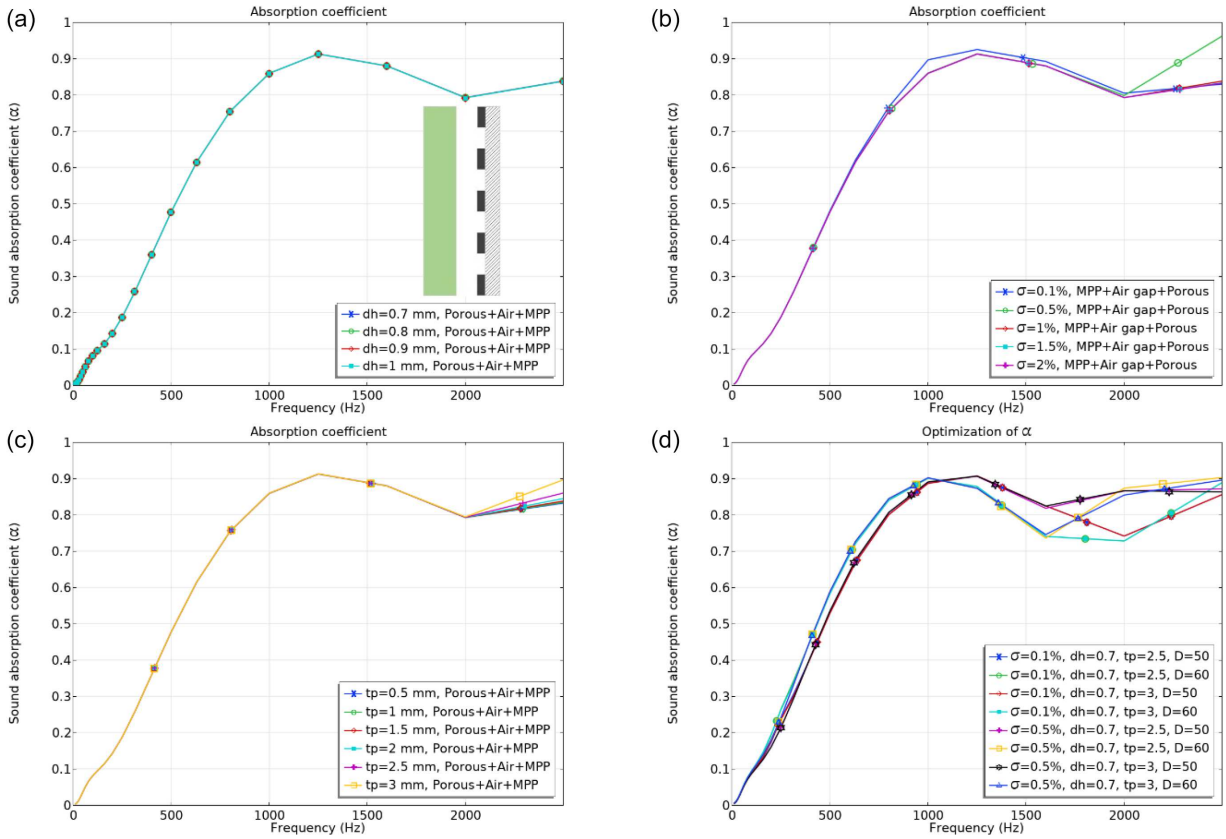

offer an ideal balance for wideband sound absorption. At higher frequencies, the results reveal an inverse relationship: the largest air gap (60 mm) exhibits a lower SAC, while smaller air gaps demonstrate higher absorption coefficients. Figure 11 depicts the fifth configuration (PAM) of sound absorption performance of multilayered structures consisting of a porous material as the first layer, an air gap in the middle, and the MPP in the third layer.

In this configuration, the air gap and MPP do not significantly influence the SAC. Similar to the first configuration, variations in hole diameter, perforation ratio, and panel thickness exhibit negligible effects on SAC, indicating that the MPP layer does not meaningfully contribute to the system's acoustic performance. Instead, the porous material remains the dominant absorber, with its intrinsic properties governing the overall absorption characteristics. A 4 cm thick porous material demonstrates superior absorption performance, especially in the mid- to high-frequency range, achieving an average SAC between 0.7 and 0.9. However, the absence of any noticeable performance enhancement with the addition of MPP suggests that this structural configuration is acoustically ineffective. The consistent behavior across all cases further implies that the MPP functions merely as a passive layer, without actively enhancing sound dissipation. However, compared to the first configuration, there is a notable improvement in the mid- to high-frequency range (above 1000 Hz), where the SAC increased from 0.65 to 0.9. This enhancement is primarily attributed to the 4 cm thick porous material, which demonstrates superior absorption in this frequency range. Despite this improvement, the lack of performance enhancement due to the MPP layer suggests that the current structural configuration remains acoustically ineffective, with the MPP acting merely as a passive layer rather than actively contributing to sound dissipation. When MPP, air gap, and porous materials are combined in a structure, placing the porous material as the first layer (directly exposed to sound energy) causes the SAC to be primarily influenced by the porous material, with the air gap and MPP having only a minor effect. This occurs because porous materials generally provide higher SAC at mid to high frequencies and positioning them at the front leads to dominant absorption in these frequency ranges. In contrast, MPP layers are more efficient at absorbing low-frequency sounds. To achieve broader frequency absorption, the arrangement of MPP and porous layers should be optimized. Figure 12 illustrates the effect of cavity depth on the sixth configuration (porous–MPP–air, PMA), where the porous layer is positioned closest to the sound source, followed by the MPP and the air gap. In this configuration, the SAC exhibits a characteristic pattern, initially increasing with frequency across all air gap thicknesses, followed by a slight decrease and a subsequent rise, with distinct peaks emerging in the low-frequency range and achieving a maximum SAC of 1.0. Notably, below 1000 Hz, the air gap thickness plays a crucial role: as the thickness increases, the absorption peaks shift toward mid- and high-frequency regions, indicating improved low-frequency absorption performance. However, beyond 1000 Hz, the influence of air gap thickness becomes negligible, with all configurations demonstrating a similar upward absorption trend, irrespective of the gap thickness. The key distinction between the low-frequency and mid- to high-frequency behaviors lies in this dependency on the air gap; while low-frequency absorption is sensitive to

Figure 12
Effect of air cavity depths on the sound absorption coefficient of porous–MPP–air structure, sixth configuration (PMA)

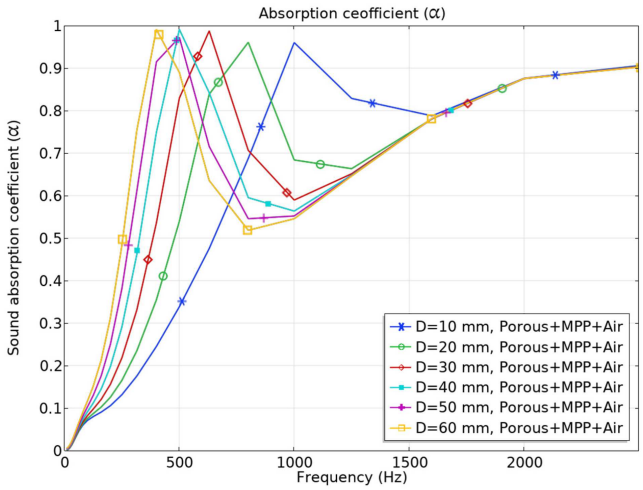

variations in air gap thickness, resulting in peak shifts, mid- to high-frequency absorption remains largely unaffected by such changes.

Figure 13 depicts the sixth configuration (PMA) of sound absorption performance of multilayered structures consisting of a porous material as the first layer, the MPP as a second layer, and an air gap in the third layer. In this configuration, the hole diameter of the MPP within the range of 0.7–1 mm demonstrates no substantial impact on the SAC (Figure 13(a)). Regarding the perforation ratio, Figure 13(b), an increase in perforation percentage leads to a shift of the absorption peak toward mid frequencies, with a maximum SAC of 1.0 at 500 Hz for the 1% perforation ratio. Beyond 1000 Hz, the perforation ratio no longer influences the SAC, and all curves exhibit a consistent upward trend, peaking at 0.9 at higher frequencies. Interestingly, the 0.1% perforation ratio sample displays a SAC of 0.55 at 250 Hz, decreases to 0.25, and subsequently rises to 0.9 at 2500 Hz, highlighting its unique absorption behavior. In terms of panel thickness (Figure 13(c)), increasing thickness enhances low-frequency absorption, with the 0.5 mm thick MPP showcasing a broader absorption range compared to the 3 mm thickness. Notably, the 1.5 mm thick sample achieves the highest SAC of 1.0 in the low-frequency region (500 Hz). After reaching this peak, all thicknesses exhibit a decline, followed by a second rise beginning at 1000 Hz. Beyond this point, thickness variations have no significant effect, with all thicknesses showing a similar upward trend, peaking at 0.9 above 2000 Hz. Based on the parametric investigation graph, the optimal configuration is achieved with an MPP thickness of 3 mm, a hole diameter of 0.8 mm, a perforation ratio of 1%, and an air gap of 60 mm. This combination yields the highest SAC, reaching 0.97 in the low-frequency range and 0.9 in the high-frequency region, indicating excellent broadband sound absorption performance.

Figure 13
Sound absorption performance of sixth configuration (PMA) with varying air gap thicknesses (10–60 mm): (a) effect of hole diameter, (b) effect of perforation ratio, (c) effect of thickness of MPP, (d) parametric investigation

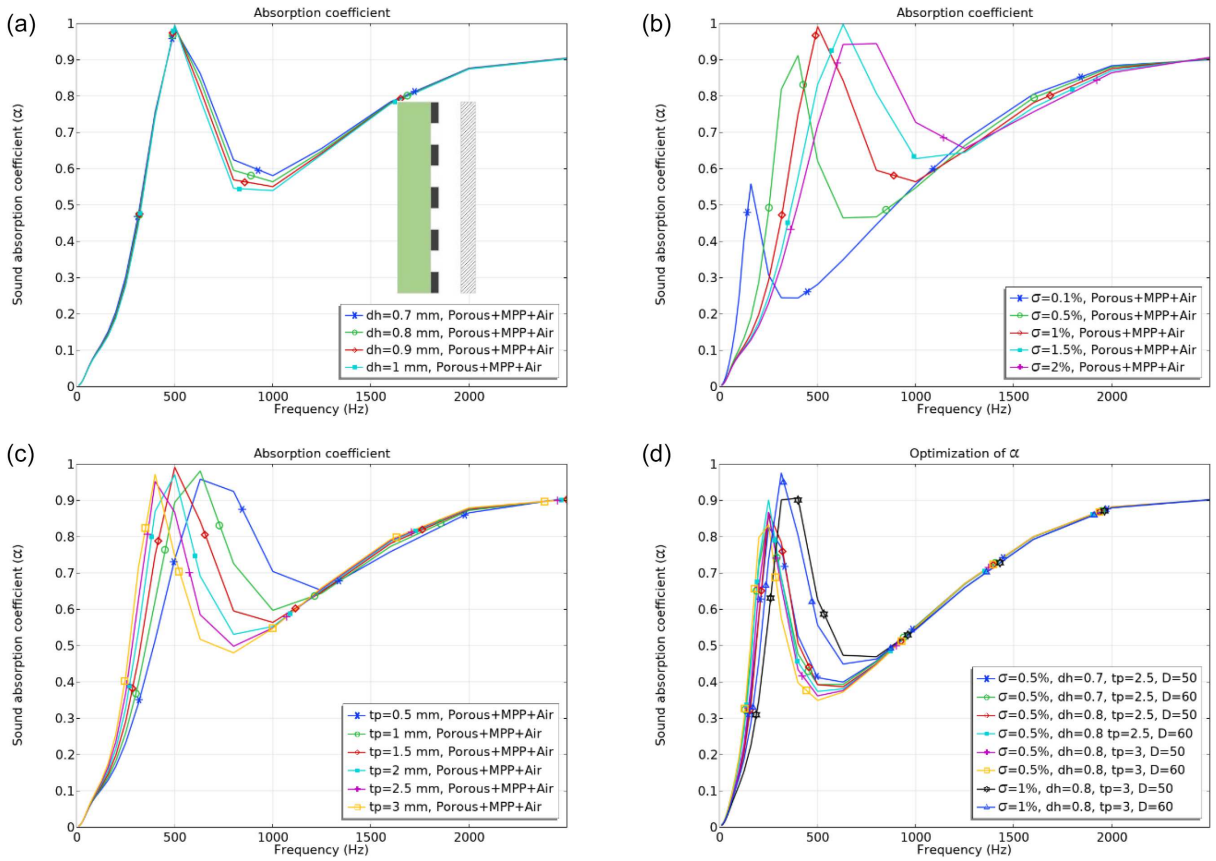

Figure 14
Comparison of experimental results with predictions from the Delany–Bazley model and Modified Delany–Bazley model for sound absorption properties

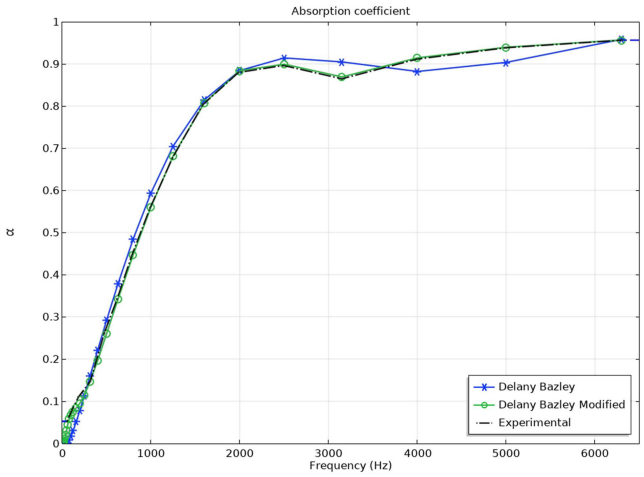

4.4. Experimental and modeling comparison

Figure 14 presents a comparative analysis of experimental data and theoretical predictions obtained from the Delany–Bazley model and the Modified Delany–Bazley model for sound absorption properties. This comparison serves to evaluate the predictive accuracy of these models in capturing the real acoustic behavior of the tested material. The dataset consists of three curves: the Delany–Bazley model (blue line with crosses), the Modified Delany–Bazley model (green line with circles), and the experimental results (black dashed line). As illustrated in the figure, the SAC increases sharply at lower frequencies, reaching approximately 0.9 below 2000 Hz, before peaking and subsequently stabilizing. Among the models, the Modified Delany–Bazley model exhibits a strong correlation with experimental results, particularly beyond the peak region, demonstrating its improved predictive capability. Conversely, the original Delany–Bazley model shows noticeable deviations at higher frequencies (above 2000 Hz), indicating certain limitations in its ability to accurately represent the material's acoustic response. At lower frequencies, both models exhibit reliable performance in predicting sound absorption behavior. However, as frequency increases, discrepancies become evident, particularly with the original Delany–Bazley model, suggesting that it may not fully account for the complex acoustic interactions within the material. In contrast, the Modified Delany–Bazley model aligns more closely with experimental findings, reinforcing its accuracy, reliability, and potential applicability in future acoustic modeling and material characterization studies.

The Modified Delany–Bazley model closely aligns with experimental findings, proving to be a more precise and dependable method for predicting the sound absorption characteristics of NFRCs. These composites possess distinctive porous structures, fiber–matrix interactions, and density variations, all of which significantly impact their acoustic properties. By incorporating these factors, the Modified Delany–Bazley model offers a more accurate representation of NFRC behavior compared to the traditional model. Its improved predictive capability and adaptability make it an ideal choice for NFRC analysis, facilitating more reliable simulations and optimizations for applications in automotive, construction, and aerospace industries, where effective sound absorption is essential.

5. Conclusion

The thickness of the porous material significantly influences sound absorption, particularly in the mid- to high-frequency range [44]. In the high-frequency range, the porous layer directly exposed to sound dominates the acoustic response, with its intrinsic properties such as tortuosity, porosity, and flow resistivity ensuring consistent and robust energy dissipation. However, at lower frequencies, the porous layer alone is less effective, as its thickness may not be sufficient to establish the necessary quarter-wavelength resonance. This emphasizes the importance of combining the porous material with complementary elements, such as air gaps or MPPs, to improve low-frequency absorption [45]. At low frequencies, increasing the air gap thickness enhances SAC [46] by shifting the resonance frequency lower, improving acoustic compliance, and amplifying absorption of long-wavelength sound waves. Configurations with the air gap positioned as the last layer further maximize resonance effects, making them particularly effective for low-frequency absorption. When the air gap is placed as the second layer, the resonance effect weakens slightly, leading to reduced SAC in this range. In the mid-frequency range, thicker air gaps and configurations with the air gap as the last layer maintain stronger interactions between the MPP and the cavity, resulting in superior SAC. Conversely, positioning the air gap as the second layer provides a smoother, more balanced absorption curve but slightly reduces mid-frequency performance. At high frequencies, the air gap's impact diminishes, as the porous layer dominates through viscous and thermal dissipation. Overall, thicker air gaps and configurations with the air gap as the last layer provide superior low- and mid-frequency absorption. MPP parameters such as perforation ratio, hole diameter, and thickness significantly influence the SAC curve, especially at low-to-mid frequencies. Increasing the perforation ratio boosts low-frequency absorption by enhancing acoustic interaction and resonance effects, though higher ratios (1–2%) slightly reduce mid- to high-frequency absorption due to lower impedance matching. Smaller hole diameters (0.7 mm) improve low-frequency absorption through stronger viscous effects, while larger diameters (0.8–1 mm) shift resonance to higher frequencies. Thinner MPPs (0.5 mm) enhance low-frequency absorption [47], whereas thicker MPPs (2.5–3 mm) provide more uniform mid-frequency absorption. Combining optimal MPP parameters with appropriate porous material thickness and air gap ensures broadband absorption with minimal resonance peaks [48]. The configuration with an MPP layer, porous material, and varying air gap thicknesses achieves superior sound absorption across low and high frequencies. The MPP targets low-to-mid frequencies via viscous and thermal dissipation, while the porous layer enhances high-frequency absorption through friction and scattering. The air gap acts as a resonance cavity, with larger gaps (e.g., 60 mm) improving low-frequency performance by tuning resonance. This design ensures effective impedance matching, reducing reflection and maximizing energy dissipation. The combined effects create a multi-resonant system, offering broad-spectrum absorption with minimal peaks and dips, outperforming alternative configurations. The configuration with the MPP as the first layer, porous material second, and a variable air gap third outperforms others due to its multilayered synergy. The MPP efficiently absorbs low-to-mid frequencies through viscous and thermal losses while reducing surface reflection. The porous layer enhances

high-frequency absorption via scattering and friction, and the air gap acts as a tunable cavity, boosting low-frequency absorption by optimizing resonance. This arrangement ensures better impedance matching, broader frequency coverage, and fewer resonance dips, offering superior noise mitigation compared to other designs.

Recommendations

The field of acoustic materials and sound absorption presents numerous opportunities for innovative research and development. Based on the findings and configurations analyzed, future researchers can focus on the following key areas:

1) Hybrid Configurations: Investigate hybrid acoustic systems combining the functionally graded materials, MPPs, and multilayer porous structures. Such configurations hold the potential to achieve broad-spectrum absorption while minimizing resonance effects, with applications in automotive, aerospace, and architectural acoustics.
2) Computational Optimization Techniques: Leverage advanced computational tools, including finite element modeling and machine learning, to optimize configurations involving MPPs, air gaps, and porous layers for superior SAC performance.
3) Advanced Porous Materials: Develop and investigate novel porous and natural fiber materials with optimized parameters such as porosity, tortuosity, and flow resistivity to enhance sound absorption performance across a wide frequency spectrum. Emphasis can be placed on sustainable solutions using bio-based, recycled, or nanomaterials.
4) Dynamic and Adaptive Acoustic Systems: Explore the design and implementation of dynamic systems capable of adapting their acoustic properties in real time to address varying noise conditions. This could include smart materials or active noise control technologies for enhanced performance.

Ethical Statement

This study does not contain any studies with human or animal subjects performed by any of the authors.

Conflicts of Interest

The authors declare that they have no conflicts of interest to this work.

Data Availability Statement

Data are available from the corresponding author upon reasonable request.

Author Contribution Statement

Majid Mohammadi: Conceptualization, Methodology, Software, Validation, Formal analysis, Investigation, Resources, Data curation, Writing – original draft, Writing – review & editing, Visualization, Supervision, Project administration. **Armin Hashemi:** Software.

References

[1] Rahayu, A. M. K., Triwanto, T., Arantxha, S. A. N., & Astuti, R. Y. (2025). The role of law enforcement and government policies in combating air pollution for a sustainable environment. *JIHK*, *6*(2), 211–226. https://doi.org/10.46924/jihk.v6i2.255

[2] Adbi, A., Agarwal, S., & Ghosh, P. (2025). Urban noise pollution and learning in developing economies. *Nature Cities*, *2*(1), 6–7. https://doi.org/10.1038/s44284-024-00189-4

[3] Lercher, P., Dzhambov, A. M., & Waye, K. P. (2025). Environmental perceptions, self-regulation, and coping with noise mediate the associations between children's physical environment and sleep and mental health problems. *Environmental Research*, *264*. 120414. https://doi.org/10.1016/j.envres.2024.120414

[4] Karimzadegan, H. A. S. A. N., & Thagipor, R. (2025). Investigation of noise pollution and its effects on blood pressure in sawmills in Bandar Anzali. *Journal of Environmental Science Studies*, *9*(4), 9312–9302.

[5] Ikpekha, O. W., & Simms, M. (2025). Effect of acoustic absorber type and size on sound absorption of porous materials in a Full-Scale reverberation chamber. *Acoustics*, *7*(1), 3. https://doi.org/10.3390/acoustics7010003

[6] Megha, K. B., Anvitha, D., Parvathi, S., Neeraj, A., Sonia, J., & Mohanan, P. V. (2025). Environmental impact of microplastics and potential health hazards. *Critical Reviews in Biotechnology*, *45*(1), 97–127. https://doi.org/10.1080/07388551.2024.2344572

[7] Lupescu, D., Robert, M., & Elkoun, S. (2025). Development of acoustic insulating carpets from milkweed fibers using air-laid spike process. *Fibers*, *13*(1), 4.

[8] Skosana, S. J., Khoathane, C., & Malwela, T. (2025). Driving towards sustainability: A review of natural fiber reinforced polymer composites for eco-friendly automotive lightweighting. *Journal of Thermoplastic Composite Materials*, *38*(2), 754–780.

[9] Mohammadi, M., Ishak, M. R., & Sultan, M. T. H. (2024). Exploring chemical and physical advancements in surface modification techniques of natural fiber reinforced composite: A comprehensive review. *Journal of Natural Fibers*, *21*(1), 2408633. https://doi.org/10.1080/15440478.2024.2408633

[10] Shao, H., Chen, W., & Jiang, D. (2025). Broaden noise reduction range in low frequency by a HR+ MPP structure based on impedance matching method. *Applied Acoustics*, *232*, 110572. https://doi.org/10.1016/j.apacoust.2025.110572

[11] Garg, N., Gautam, C., Rab, S., Wan, M., Agarwal, R., & Yadav, S (Eds.). (2024). *Handbook of vibroacoustics, noise and harshness*. Singapore: Springer Nature. https://doi.org/10.1007/978-981-97-8100-3

[12] Peng, X., Xie, X., Yang, W., Chen, M., Wang, Y., & Xu, L. (2025). Low frequency sound absorption metasurface optimization design method based on deep learning. *Applied Acoustics*, *231*, 110446. https://doi.org/10.1016/j.apacoust.2024.110446

[13] Mohammadi, M., Ishak, M. R., Hameed Sultan, M. T., & Zainudin, E. S. (2025). Cutting-edge innovations in sound absorption properties of natural fiber reinforced polylactic acid composites. *Journal of Reinforced Plastics and Composites*. https://doi.org/10.1177/07316844251352718

[14] Ravikiran, A., George, R., Subramanian, K. R. V., & Kallannavar, U. S. (2025). High energy processing of natural fiber composites. *Next Research*, *2*(1), 100113. https://doi.org/10.1016/j.nexres.2024.100113

[15] Železnik, A., Čurović, L., & Prezelj, J. (2025). Sustainable sound absorption using shredded plastic particles: Adjusting low-frequency acoustic performance with particle size. *Journal*

of Low Frequency Noise, Vibration and Active Control, *44*(2), 1139–1150. https://doi.org/10.1177/14613484251314934

[16] Feng, Z., Xu, X., Wen, S., Wu, Z., & Li, F. (2025). Enhanced sound absorption properties of a semi-open underwater periodic acoustic metamaterial. *Composite Structures*, *354*, 118831. https://doi.org/10.1016/j.compstruct.2024.118831

[17] Qian, Y., Li, B., & Wei, Y. (2025). Bandwidth narrowing effect in higher-order frequency bands of microperforated panel absorbers: analysis and suppression strategies. *Journal of Vibration Engineering & Technologies*, *13*(1), 24. https://doi.org/10.1007/s42417-024-01595-7

[18] SheikhMozafari, M. J. (2024). Enhancing sound absorption in micro-perforated panel and porous material composite in low frequencies: A numerical study using FEM. *Sound & Vibration*, *58*, 81–100. https://doi.org/10.32604/sv.2024.048897

[19] Zhang, P. F., Li, Z. H., Zhou, Y. J., Zhang, Q. F., Liu, B., Liu, F., . . . , & Bai, P. K. (2025). Improved sound absorption with 3D-printed micro-perforated sandwich structures. *Journal of Materials Research and Technology*, *34*, 855–865.

[20] Mohammadi, M., Ishak, M. R., Sultan, M. T. H., & Zainudin, E. S. (2025). A comprehensive review of factors influencing the sound absorption properties of micro-perforated panel structures. *Journal of Vibration Engineering & Technologies*, *13*(5), 319. https://doi.org/10.1007/s42417-025-01849-y

[21] Zhao, Y., Lou, H., RONG, N., & Min, H. (2024). Random incidence absorption characteristics and parameterized design of micro-perforated panel absorbers with parallel-arranged backing cavities at different depths. *INTER-NOISE and NOISE-CON Congress and Conference Proceedings*, *270*(10), 1937–1946. https://doi.org/10.3397/IN_2024_3106

[22] Min, H., Lou, H., & Zhao, Y. (2025). Optimization of parallel coiled cavities of different depths in microperforated panel sound absorbers. *Scientific Reports*, *15*(1), 1401. https://doi.org/10.1038/s41598-025-85171-3

[23] Tayong, R. B. (2025). *Panels for Sound Absorption. Acoustical Engineering-The Intricate World of Sound Technology: The Intricate World of Sound Technology* (pp.63) Intechopen. https://doi.org/10.5772/intechopen.1004684

[24] Anaghraj, R., Mahesh, K., & Mini, R. S. (2025). Low-frequency acoustic performance of a microperforated panel integrated coiled-up space absorber with subwavelength thickness. *Journal of Vibration and Acoustics*, *147*(1), 011003. https://doi.org/10.1115/1.4067285

[25] Sheikhmozafari, M. J., Ahmadi Asour, A., & Hajinejad, S. (2024). Enhancing high-frequency bandwidth in MPP-porous material composite absorbers: A numerical simulation approach for optimal parameter selection. *Journal of Occupational Health and Epidemiology*, *13*(2), 119–131. https://doi.org/10.61186/johe.13.2.119

[26] Beheshti, M. H., Khavanin, A., Jafarizaveh, M., & Tabrizi, A. (2024). A novel acoustic micro-perforated panel (MPP) based on sugarcane fibers and bagasse. *Journal of Materials Science: Materials in Engineering*, *19*(1), 35. https://doi.org/10.1186/s40712-024-00173-9

[27] Nandanwar, A., Kiran, M. C., & Varadarajulu, K. C. (2017). Influence of density on sound absorption coefficient of fibre board. *Open Journal of Acoustics*, *7*(1), 1–9. https://doi.org/10.4236/oja.2017.71001

[28] Lyu, L., Pan, J., Zhang, D., Qian, Y., Gao, Y., & Zhou, X. (2025). Design, preparation, and analysis of the acoustic performance of waste hemp/PLA fiber sound-absorbing composites with different bionic structures. *Industrial Crops and Products*, *223*, 120145. https://doi.org/10.1016/j.indcrop.2024.120145

[29] Bainamndi, J. D., Siryabe, E., Ntamack, G. E., Yamigno, S. D., & Maréchal, P. (2024). Assessing acoustic performance of building material: A finite element model for 3D printed multilayer micro-perforated panels with compressed earth blocks. *Building Acoustics*, *31*(3). 247–267. https://doi.org/10.1177/1351010X241265241

[30] Patil, C., Ghorpade, R., & Askhedkar, R. (2024). Analysing the impact of 3D-printed perforated panels and polyurethane foam on sound absorption coefficients. *Modelling*, *5*(3), 969–989. https://doi.org/10.3390/modelling5030051

[31] Arjunan, A., Baroutaji, A., Robinson, J., Vance, A., & Arafat, A. (2024). Acoustic metamaterials for sound absorption and insulation in buildings. *Building and Environment*, *251*.

[32] Min, H., Lou, H., & Zhao, Y. (2024). Acoustic properties of a micro-perforated muffler with parallel-arranged cavities of different depths. *Building and Environment*, *261*, 111728. https://doi.org/10.1016/j.buildenv.2024.111728

[33] Chen, Y., Yu, K., Fu, Q., Zhang, J., Lu, X., Du, X., & Sun, X. (2024). A broadband and low-frequency sound absorber of sonic black holes with multi-layered micro-perforated panels. *Applied Acoustics*, *217*, 109817. https://doi.org/10.1016/j.apacoust.2023.109817

[34] Zhao, Y., Min, H., & Rong, N. (2024). Random incidence sound absorption of micro-perforated panel absorbers backed with parallel-arranged cavities of different depths. *Applied Acoustics*, *222*, 110064. https://doi.org/10.1016/j.apacoust.2024.110064

[35] Qin, M., Wang, J., Deng, Q., & Cai, J. (2024). Insert loss experiment and acoustic impedance theoretical study on the noise barrier with MPP-QRD top structure. *Applied Acoustics*, *221*, 109996. https://doi.org/10.1016/j.apacoust.2024.109996

[36] Taban, E., Khavanin, A., Ohadi, A., Putra, A., Jafari, A. J., Faridan, M., & Soleimanian, A. (2019). Study on the acoustic characteristics of natural date palm fibres: Experimental and theoretical approaches. *Building and Environment*, *161*, 106274. https://doi.org/10.1016/j.buildenv.2019.106274

[37] Maa, D. Y. (1998). Potential of microperforated panel absorber. *The Journal of the Acoustical Society of America*, *104*(5), 2861–2866. https://doi.org/10.1121/1.423870

[38] Delany, M. E., & Bazley, E. N. (1970). Acoustical properties of fibrous absorbent materials. *Applied Acoustics*, *3*(2), 105–116. https://doi.org/10.1016/0003-682X(70)90031-9

[39] Tao, Z., Zhang, B., Herrin, D. W., & Seybert, A. F. (2005). *Prediction of sound-absorbing performance of micro-perforated panels using the transfer matrix method (No. 2005-01-2282)*. SAE Technical Paper. https://doi.org/10.4271/2005-01-2282

[40] Berardi, U., & Iannace, G. (2015). Acoustic characterization of natural fibers for sound absorption applications. *Building and Environment*, *94*, 840–852. https://doi.org/10.1016/j.buildenv.2015.05.029

[41] Cox, T., & d'Antonio, P. (2016). *Acoustic absorbers and diffusers: Theory, design and application*. USA: CRC Press.

[42] Miki, Y. (1990). Acoustical properties of porous materials-Modifications of Delany-Bazley models. *Journal of the Acoustical Society of Japan (E)*, *11*(1), 19–24. https://doi.org/10.1250/ast.11.19

[43] Komatsu, T. (2008). Improvement of the Delany-Bazley and Miki models for fibrous sound-absorbing materials. *Acoustical*

Science and Technology, *29*(2), 121–129. https://doi.org/10.1250/ast.29.121,

[44] SheikhMozafari, M. J., Taban, E., & Attenborough, K. (2026). Porous sound absorbing materials from natural sources: Data and modelling. *Applied Acoustics*, *243*, 111162. https://doi.org/10.1016/j.apacoust.2025.111162

[45] Rezaieyan, E., Taban, E., Berardi, U., Mortazavi, S. B., Faridan, M., & Mahmoudi, E. (2024). Acoustic properties of natural fiber reinforced composite micro-perforated panel (NFRC-MPP) made from cork fiber and polylactic acid (PLA) using 3D printing. *Journal of Building Engineering*, *84*, 108491. https://doi.org/10.1016/j.jobe.2024.108491

[46] Erol, M., & Aydemir, H. (2025). Effect of air gap on sound absorption in layered composite structures produced of sustainable materials. *The Journal of The Textile Institute*, *116*(5), 799–807. https://doi.org/10.1080/00405000.2024.2356274

[47] Yeang, W. Y., Halim, D., Yi, X., & Chen, H. (2024). On improving low-frequency sound absorption using a compound microperforated panel backed by a panel-type resonator with tuned multi-frequency resonators. *Journal of Sound and Vibration*, *570*, 118134. https://doi.org/10.1016/j.jsv.2023.118134

[48] Liu, C. R., Wu, J. H., Yang, Z., & Ma, F. (2020). Ultra-broadband acoustic absorption of a thin microperforated panel metamaterial with multi-order resonance. *Composite Structures*, *246*, 112366. https://doi.org/10.1016/j.compstruct.2020.112366

How to Cite: Mohammadi, M., & Hashemi, A. (2026). Numerical Investigation of Low-Frequency Sound Absorption in Micro-Perforated Panel–Porous Composite Structures. *Archives of Advanced Engineering Science*, 1–16. https://doi.org/10.47852/bonviewAAES62028673